Mechanics of Advanced Composite Structures

Journal homepage: https://macs.semnan.ac.ir/

Semnan University

ISSN: 2423-7043

Structural Analysis of Composite Material Disk Brakes

Ekhlas Edan Kader [a], Akram Mahdi Abed [b], Saša Milojević [c], Blaža Stojanović [c]

[a] *Engineering Materials Department, University of Diyala, Diyala, Iraq*
[b] *Mechanical Engineering Department, University of Diyala, Diyala, Iraq*
[c] *Faculty of Engineering University of Kragujevac, University of Kragujevac, Serbia*

A R T I C L E I N F O

Article history:

Received:
Revised:
Accepted:

Keywords:

Keyword 1; hybrid composite
Keyword 2; disk brake
Keyword 3; Minitab
Keyword 4; Finite element

.

A B S T R A C T

The superior properties of composite materials compared to traditional materials led to significant attention in the development of disk brake manufacturing. In many industrial and automotive applications where performance and durability are dominant, disk brakes are critical components. This study investigates hybrid brake pads of Aluminum-based composites made by adding different percentages of silicon carbide (15% and 20% SiC) and zinc oxide (10%, 15%, and 20% ZnO). The goal was to find a combination that improves brake efficiency, reduces wear, and increases service life. Wear tests and hardness measurements were carried out according to ASTM standards. The experimental results were analyzed using Minitab 19 with a Design of Experiments (DOE) method to study how wear changes over time under different loads. Time-series trend analysis was also used to visualize how the specific wear rate develops, while the residuals-versus-fitted-values plot was used to assess the regression model and validate its assumptions. The fitted values represent the predicted specific wear rate over time. Additionally, a residuals-versus-observation-order plot was used to illustrate the correlation of these differences over time. The results showed that sample A5 had the best wear resistance and certified A5 as the optimum structural stability over time composite sample. The hardest samples were A2 and A5. Based on these findings, the best composite formulation was selected for further analysis using ANSYS 2022-R1. In ANSYS, a static structural analysis was performed to evaluate stress, strain, deformation, and elastic energy. The thermal analysis examined heat distribution, heat generation, and heat flux in the hybrid composite material. The numerical results provided serious understandings in which stress levels are significantly lower at the outer surfaces compared to the inner regions**.** The outer surfaces exhibit a uniform distribution of average heat flux. Directional heat flux shows a slight increase near the inner radius, the disk protrusions, and edges. These findings helped to understand how the optimal composite behaves under braking conditions.

1. Introduction

The sharp decline in energy resources necessitated the investigation of new materials for efficient use in structural applications.

In the automobile industry, safety is primarily about the brakes. It retards the vehicle's moving members by applying frictional forces. The brake plate plays a significant role in absorbing kinetic energy and dissipating heat.

*** Corresponding author.**
E-mail address: ekhlasedan_eng@uodiyala.edu.iq

Cite this article as:
. *Mechanics of Advanced Composite Structures*, 12(1), pp. xx-xx

The excessive heat condition makes the drum brake insufficient, as the rider must apply more effort to brake, and the brake should be adjusted regularly.

There are many types of brakes; the most common one is the disk brake. Frederick William patented the first disk -type automobile disk brake in 1902. Frederick's disk brake failed because it was made of copper [1].

In a disk brake, a flat metal rotor disk spins with the wheel. The disk pad is squeezed by the Caliper when the brake is applied to stop or retard the motion (Pathak, Anshul Choudhary, and Jain, no date). Pascal's law is applied to operate the disk brake. Entering the fluid into the cylinder bore of the Caliper assembly through the brake hoses and pushes the Caliper piston[2].

At the same time, the piston ring rolls with the piston, pushing the brake pad. The brake pads stick to the brake disc during this movement, creating friction that slows or stops the brake disc and the vehicle. The piston ring pushes the Caliper piston back to the cylinder bore when the brake lever is released, then both return to their original positions. Meanwhile, the reaction spring pushes the brake pads to the first position. The master cylinder assembly spring pushes the cylinder piston back to its original position, allowing fluid to flow [3].

Traditional disk brake material is cast iron, though it has limitations in terms of weight, corrosion resistance, and wear.

The development in the structural industry, especially in the automotive industry, makes the use of lightweight, strong, safer, and low-cost materials a considered demand. Improving vehicle toughness and safety, and reducing cost and fuel consumption without increasing vehicle weight, can be achieved by introducing composite materials to the manufacturing of disk brakes [4].

Composite materials imply that more than one material is united on an infinitesimal scale to produce a beneficial material, while the individual constituents keep their characteristic. Many material characteristics can be combined to obtain the required properties of the resulting composite that cannot be achieved with alloys. Choosing the appropriate matrix and reinforcement is the most important step in applying composite materials to a specific application [5]

Metal Matrix Composite (MMC) has a noteworthy role in manufacturing applications, mainly in lightweight materials. Using an Aluminum-based metal matrix composite as a braking material is an efficient and practical choice. The attractive properties that make Aluminum a more competitive material than cast iron are its high specific strength and stiffness, excellent formability, good thermal and electrical conductivities, high ductility and weldability, excellent atmospheric corrosion resistance, controlled thermal expansion coefficient, and improved abrasion and wear resistance. The drawbacks of Aluminum are its low resistance to wear and its large thermal deformation. Introducing reinforcement ceramic materials, such as SiC and ZnO, enhanced those drawbacks. Ceramics have the characteristic property of no slip planes and do not deform when force is applied. Silicon carbide is a competent ceramic material for use as a reinforcing component in Aluminum or its alloys.

A high-performance ceramic material, SiC, is increasingly used in the manufacturing of disk brakes for its effective properties. SiC has the superior thermal conductivity required to dissipate heat generated during braking. Hard SiC makes it a wear-resistant material that imparts long-lasting performance with minimal wear at the disk pad and rotor surface.[6].

Additionally, ZnO plays a significant role in disk brake manufacturing by enhancing performance and durability. It is an ideal additive due to its unique properties, providing stability, thermal conductivity, and frictional characteristics, which are important for efficient braking.

ZnO can enhance brake performance by improving the thermal conductivity of the friction material. Dissipating the heat generated during braking with ZnO helps prevent brake fade and ensures reliable stopping control, even under high-stress conditions. ZnO promotes adhesion between the friction material and the brake rotor, reducing wear and extending the lifespan of the braking system [7].

Aluminum base, reinforced with a SiC and ZnO composite, disk brakes weigh less than cast-iron and structural-steel disk brakes.

Many experimental and analytical studies investigate replacing traditional disk brake materials with composite materials.

Piotr GRZEŚ investigated the temperature fields in a solid disk brake during short, emergency braking. Performing the transient thermal analysis of disk brakes in a single brake application using the numerical simulation of the parabolic heat conduction equation for a two-dimensional model. The evolution of the disk's rotational speed and contact pressure, with specific material properties, strongly affects the disk brake temperature fields in time, as shown in the results [8].

Pohane Rajendra developed a 3D F.E. model for static and transient structural analysis of the brake pad and disk. The solid and ventilated disc performance is compared using the same material properties and constraints. The equivalent von Mises stresses and thermal stresses at the disk-pad interface were analyzed using FE analysis[9].

Prashanth Banakar& H.K. Shivananda investigated the effect of fiber orientation of laminates to determine material specifications. The hand layup process was used to obtain the laminates, which were cut to meet ASTM standards. The experimental tests were tensile and flexural strength. The experimental results showed that the mechanical properties of laminated polymer composites depend on fiber orientation[10].

Lalit N. Wankhade et al. prepared Aluminum metal matrix reinforced with 0, 2.5, and 5% SiC composite using the stir casting method. The disk method was used to analyze the composite's wear behavior. The design of experiments (DOE) and ANOVA analysis were performed using Minitab TM software. The maximum wear loss was observed in the 0 and 5% SiC samples. SiC increases hardness and compressive strength, as indicated by experimental results[11].

Abd Rahim Abu-Bakar et al. studied the distribution of contact pressure of a solid disk brake due to structural modifications. The four contact analysis models are evaluated for complexity before modification. Different contact pressure distributions obtained from these four models help design engineers achieve uniform pressure distribution and longer life[12].

Huajiang Ouyang et al. used F.E. to investigate the contact pressure distribution under the influence of the surface roughness of a real disk brake. Measured data, along with the F.E. result, were used to predict the contact pressure. The study includes the effects of wear and thermal conditions on the contact pressure distribution and squeal generation in the assembly [13].

Khalid Mahmood Ghauri and Liaqat Ali studied the reinforcement of Aluminum with SiC. Aluminum and SiC have densities close to each other, making them the best composite material with good strength and heat conductivity. Al/SiC MMC was synthesized by stir casting, with silicon carbide particles at 5, 10, 15, 25, and 30% reinforcing the Aluminum matrix. Mechanical test results showed that increasing SiC% led to increasing hardness and toughness. The 25-30% SiC showed unsteady results, which depend on the distribution of the SiC in the matrix [14].

Khalanisohil et.al.Used Aluminum and gray iron materials to model the disk brake. The study includes calculating normal, shear, and piston force. ANSYS program was used to analyze the thermal performance to explain the action force and friction effect on the proposed disk brake to work efficiently and reduce accidents.[15].

Kumar Santhosh M et al. studied the tensile, flexural, and moisture-absorption properties of composite materials made of S-glass, Carbon, and E-glass fibers. Hand lay-up techniques, as per ASTM standards, were used to prepare the specimens with thicknesses of 2 and 3 mm, and fiber orientations of 30, 45, and 60°. Changing the thickness and measuring the tensile strength of the hybrid composite was measured and compared with finite element analysis. The results showed that tensile strength strongly depends on fiber orientation and thickness. The moisture absorption increases with increasing fiber content and immersion time [16].

Kale C. studied the reduction of failure by using a nontraditional material, vanadium stainless steel. The ductility and thermal analysis were performed in static analysis of the disk rotor. The disk brake was modeled using Creo Parametric 3 and analyzed using ANSYS Workbench 15. Comparing the obtained results showed that the vanadium steel has better resistance and good temperature distribution than the traditional materials[17].

Many studies used simulation programs to predict the mechanical behavior of the composite disk brakes. Few, if any, researchers have experimentally investigated the fabrication of a composite material by combining silicon carbide with zinc oxide to reinforce Aluminum. Minitab software was used to analyze the experimental data. Time-trend analysis was used to identify the best mixture for increased wear resistance and hardness. The optimal mixture was thoroughly studied using ANSYS Workbench, with stress, strain, and deformation calculated. Additionally, the thermal behavior was evaluated by measuring the disk brake's temperature and thermal flux during operation. Using experimental tests, data analysis, and ANSYS simulations provides a clear understanding of the disk brake's behavior.

2. Experimental Works

2.1. Materials

The hybrid composite materials used in this research consist of Aluminum metal Al 6061 (150 micron) from Alpha Chemika Company (India), with a density of 2.7 g/cm^3 and an elongation at break of 10%-12%, serving as the matrix. Al reinforced with (10,15,20 wt%) ZnO with a 30-40 nm particle size from Alpha Chemika Company (India), having a density equal to 5.61 g/cm^3 and an elongation at break of less than 1%. SiC with (15,20wt%) from the Accuratus company (America), having a density equal to 3.21 and 3.22 g/cm^3 and an elongation at break of less than 1%. Table [1] shows sample names and percentages. A single reinforcement in samples A1 and A2 aimed to study the linear single variable impact of adding SiC and ZnO in disk brake performance, while samples A3 through A5 were selected to study the hybrid metal matrix composite properties. Increasing both SiC and ZnO to 20 wt %.to study the threshold of combining ceramic and oxides to decrease plastic deformation and reduce wear rate. These composite samples provide a total insight into the composite behavior to clarify the best choice for the disk brake manufacturing.

Table (1). Composite sample names and percentages

Sample percentages	**Sample names**
Aluminum +10% ZnO	A1
Aluminum+ 15% SiC	A2
Aluminum +20% SiC +10% ZnO	A3
Aluminum +20% SiC +15% ZnO	A4
Aluminum +20% SiC +20% ZnO	A5

2.2. Specimens Preparation

Specimens for experimental tests were prepared by the casting method. The Aluminum 6061 powder produced by mechanically crushing solid Aluminum 6061 at the required mixing percentage was melted at 700 °C in a graphite crucible of a high-power furnace (max. 1200 °C). After removing the dross, the weighed amount of Sic was heated to 200 °C for 30 minutes, then added to the Al 6061 by creating a whirlpool in the alloy with manual stirring. After thoroughly mixing, the ZnO powder at 10-20% was added to the mixture. The obtained composite was cast in permanent moulds.

3. Experimental Tests

Using the computer-controlled universal testing machine from Tinius Olsen Company (USA), manufacturer (USA), tester (H50KT). Loading with 0.005 m/m. minimum loading rate to perform the compression test till the breaking point on the load-deformation graph or actual failure of the sample. Compression test samples were prepared according to ASTM E9, with diameters-to-length ratios of 16 and 32.

The wear test mold was manufactured from high-strength stainless steel and designed in accordance with the international standard ASTM G99-95, with the disk material being EN 36 steel. The wear-testing samples have a diameter of 30.10 mm, and in a second case, a height of 30.10 mm. The specimens were cleaned before performing wear tests, while the weight reduction was recorded using the digital electronic balance with an accuracy of up to 0.01 g. The specific wear rate was calculated from the weight loss data. Pin-on-disk wear tests used 15,25 and35 N loads at a time (15, 25, and 35 min). The specific wear rate can be calculated using the following equation[18]:-

$$W_s = \frac{\Delta m}{\rho \cdot t \cdot v \cdot F} \quad \ldots\ldots\ldots\ldots\ldots\ldots\ldots\ldots\ldots\ldots (1)$$

W_s: Specific wear rate (mm^3/Nm),

Δm : $weight\ loss\ (g)$

ρ : the density in(g /mm3),

t : $time\ (sec)$

v : the sliding velocity in (m/s),

F : $Load\ (N)$

The experimental constraints were chosen to simulate light braking decelerating environments. The angular velocity ω = 125 rad/s and a wear test track radius r = 68 mm, the sliding velocity equal to 8.4 m/s, which is approximately 30 km/h, with the applied normal loads 15–35 N. These values imply light braking conditions in automotive engineering and outline an accurate evaluation of the hybrid composites' performance through general city driving and studying the initial stages of steady friction film development.

The Brinell hardness test is a standard method for evaluating the hardness of metals and their composites. In the test, indentation hardness is calculated using a hardened steel indenter or a carbide ball. A 10 mm diameter ball is loaded onto the test sample with a load of 2950 N according to the standards. The load should be applied gradually over 10-15 seconds of indentation time. The applied load should be maintained for a specified dwell time of 10-30 seconds to have a steady indentation. The indentation diameter must be measured from two perpendicular diagonals using an accurate device. The hardness can be calculated using the following equation [19]

$$HB = \frac{2F}{\pi D(D-\sqrt{D^2-d^2})} \quad \ldots\ldots\ldots\ldots\ldots\ldots (2)$$

Where are:

F= the applied load = 500 kg

D=10 mm, ball of fixed diameter

d= the Indenter.

Figure (1) below shows wear, hardness test samples, and wear BHN test devices.

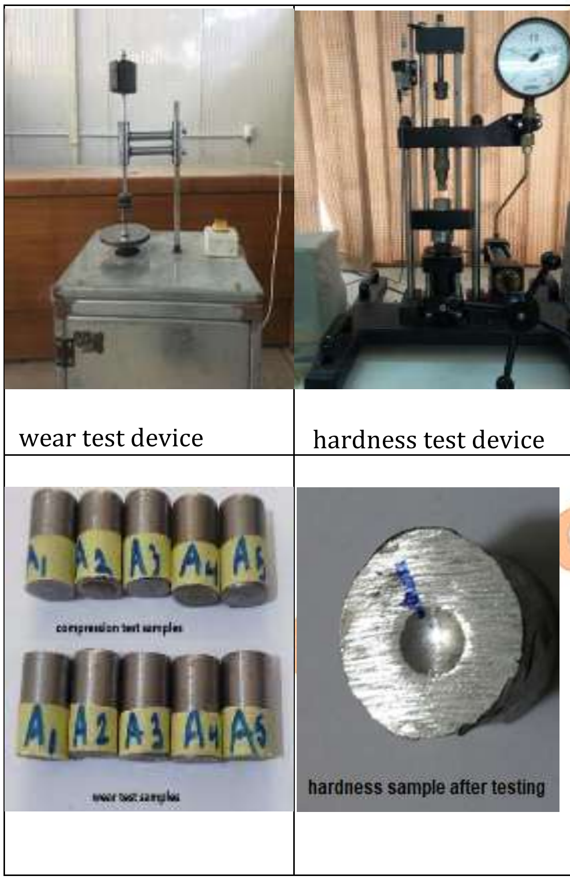

Fig. (1). The Aluminum-based hybrid composite compression, wear, BHN hardness test samples, and wear, hardness test devices.

4. Results and Discussions

The compression strength, strain, and modulus of elasticity of the composite samples are in Table [2]. Maximum strength is achieved when the Aluminum matrix is reinforced with both hard ceramic powders, SiC and ZnO, due to improved load-carrying capacity and a more uniform distribution of stress and strain within the sample, which, in turn, reduces plastic deformation.

Table 2. Compression test results of the hybrid composite samples

Sample	Max. compression strength MPa	Max. compression strain %	Modulus of elasticity GPa
A1	610	3	106
A2	645	2.5	130
A3	678	2.7	135
A4	715	2.1	140
A5	820	2	145

The specific wear rate of the composite under applied loads of 15, 25, and 35 N is shown in Fig. 2.

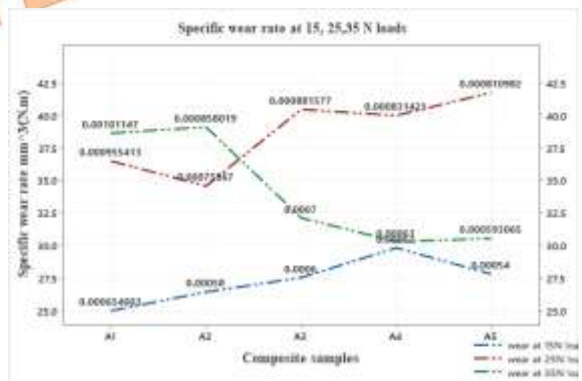

Fig. (2). Specific wear rate of the hybrid composite at 15, 25, and 35 N applied loads.

Examining Fig. 2 shows that at a load of 15N, the composite samples' specific wear rates differ slightly. Sample A5 (Aluminum + 20% SiC + 20% ZnO) resists wear better than the other samples due to the presence of hard SiC particles and the good tribological properties of ZnO, which enhance interfacial bonding and lead to better wear resistance. Sample A1 (Aluminum +15% SiC) has the worst wear resistance, which may be due to an absence of SiC content[20].

Increasing the applied load to 25N results in a noticeable increase in the specific wear rate due to greater deformation and frictional forces in the materials. The composite sample A1, with a 0.000654 specific wear rate, increased to 0.000955, and the sample A2, with a 0.000553 wear rate, increased to 0.000759. The other samples showed a change in wear rate, which may have contributed to the addition of ZnO with high friction resistance properties. Sample A3, with a 0.0006 wear rate, increased to 0.0007 and 0.000882. Sample A4, with a 0.00062 wear rate, increased to 0.00063 and 0.00083. Sample A5, with a 0.00054 wear rate, increased to 0.00081 and 0.0005931.

At an applied load of 35 N, the composite samples A1 and A2 showed a consistent increase in specific wear rate. Samples A3 and A4 showed a constant specific wear rate due to stabilization of the wear mechanism. Sample A5 shows an additional decrease in specific wear rate due to a higher amount of SiC and ZnO [21].

Figure 3 shows the specific wear rate at 15, 25, and 35 minutes of testing time. All samples showed an increase in specific wear rate with increasing test time. Increasing the time from 15-25 minutes showed a significant increase in specific wear rate, while a marginal increase in specific wear rate was noticed when the load changed from 25-35 minutes, which can be attributed to the formation of a protective layer or a change in the wear mechanism [22].

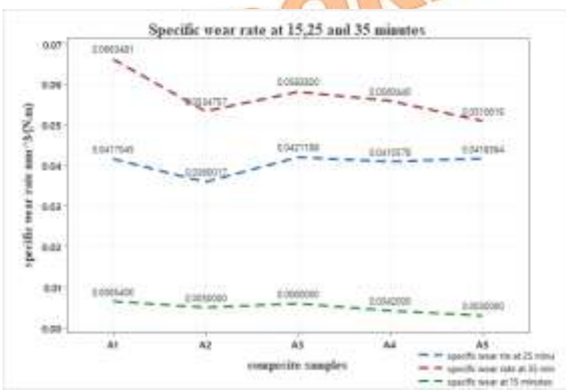

Fig. (3**)**. The specific wear rate of the hybrid composite samples at 15, 25, and 35 minutes of testing time.

To visualize the effect of time on the specific wear rate at different loads, we utilized Minitab 19's time-series trend analysis[Minitab 19 LLC, State College, PA, USA]. The primary goal of this analysis is not only to reveal basic trends but also to identify relationships that can help to understand the performance and predict future conduct of the data[23]. This predictive aspect is particularly intriguing, as it opens up possibilities for future research and applications.

The first-order approximation, linear trend analysis, was used to get the general behavior of material loss when load is applied. Linear regression provides a simple and comprehensible measure of wear rate, especially when wear rate is rather uniform over time. There are nonlinear models like power law and exponential which gave more accurate curve fitting. For comparative consideration, the slight differences don't affect the overall evaluations.

The Von Mises ANSYS stress of 1.29 MPa induced due to applied loads used in this study is adequate to provide a sensitive analysis of the DOE linear trend to visualize the SiC and ZnO effect on the wear resistance of the Aluminum-based composite.

Figure 4 shows the linear trend model for the specific wear rate at 15 minutes. The straight line declined downward with a negative slope, indicating that the specific wear rate decreased with time at a constant applied **load due to the** high load-bearing capacity of SiC, which imparts hardness, and the covering behavior of ZnO. The scattered points around the line indicate that the data are variable, with some points deviating from the trend line. This variability is due to factors not accounted for in the model, or to natural variation in the wear rate data.

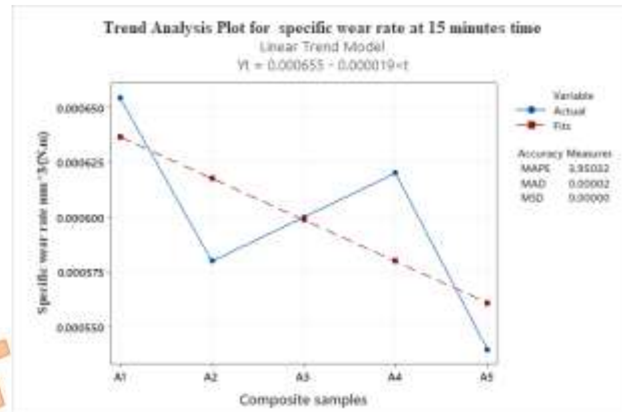

Fig. (4). The linear trend model at 15 min of the specific wear rate.

Figure (5) below shows residual plots for the specific wear rate at 15 and 15-minute testing times. The probability plot followed a straight line, indicating that the experimental test results are normally distributed and indicating a negligible error in measuring wear rate.

A residual-versus-fitted-value plot illustrates the regression model and helps validate the assumptions. The fitted values equal the predicted specific wear rate over time, showing a constant variation with accurate prediction. The residuals are the differences between the predicted and the actual specific wear rates. If the differences in wear rates are randomly distributed around a line of zero, it means that the specific wear experimental data model fits the data very well, with linearity and constant-variance residuals.

The residual versus observation order plot shows the correlation in the differences over time when the differences are randomly distributed around the zero line, without any identifiable pattern, indicating that the residuals are independent and identically distributed, meeting the model assumptions and indicating sufficient experimental data [24].

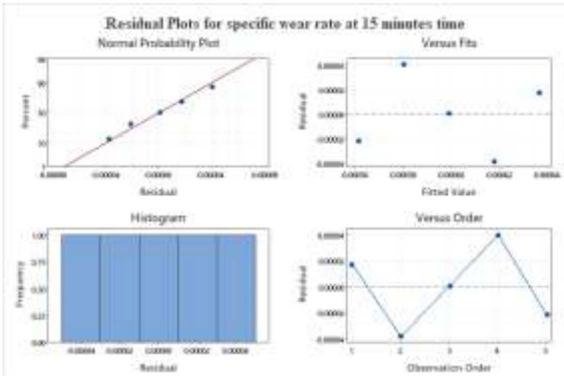

Fig. (5). The residual plots for the specific wear rate at 15 min of testing time

Figure 6 shows the linear trend model of the specific wear rate at 25 minutes. The straight line declined upward with a positive slope, indicating that the specific wear rate increased with time at a constant applied load. Increasing the testing time caused a weak connection of ceramic particles with the Al matrix, leading to particle debris. These debris particles act as ploughing particles, which increase the wear rate. The dispersed points around the line indicate that the data have variability in the overall upward direction due to the increase in loading time and showed a good prediction.

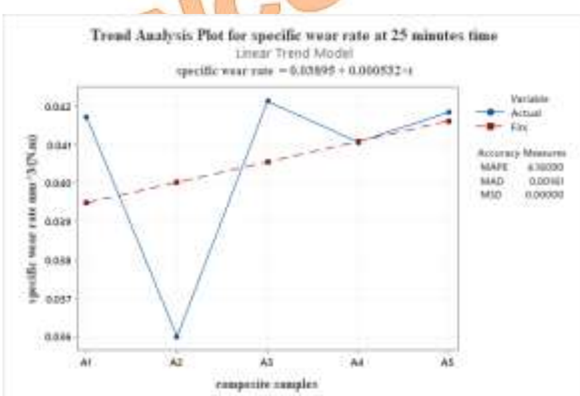

Fig. (6). The linear trend model of the specific wear rate at 25 min time

The residual plots for the specific wear rate at 25 min testing time are in Figure 7 below. The plot of the probability shows that the data are approximately linear, indicating that the experimental test results are normally distributed and with negligible errors. The residual-versus-fitted value curves show that the differences in specific wear rates are randomly distributed around the line of zero value; this means that the specific wear rate experimental data model fits the data very well, with linearity and constant-variance residuals. Since the differences are distributed randomly around the zero line without any discernible pattern, the residuals are independent and identically distributed, meeting the model assumptions in the residual-versus-observation curves [25].

Fig. (7) The residual plots for specific wear rate at 25 min testing time

The linear plot for the specific wear rate at 35 min is shown in Fig. 8. The negative slope of the straight line indicates that the specific wear rate decreased with time at a constant rate due to the formation of the tribo film due to ZnO existence and the hard particles of SiC. The spread of points around the line indicates that the variable data have an overall downward trend[26]. The addition

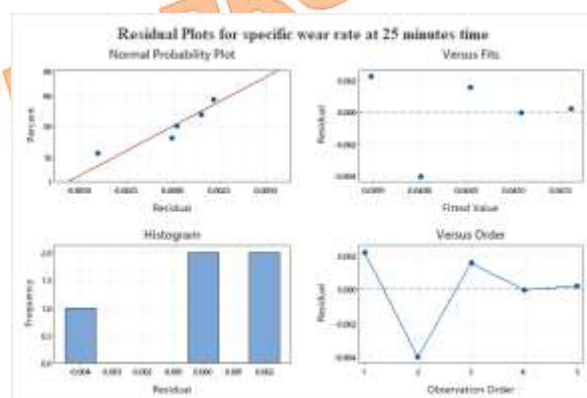

of a hybrid composite of SiC and ZnO enhances the composite's ability to withstand plastic deformation and, in turn, enhances wear resistance.

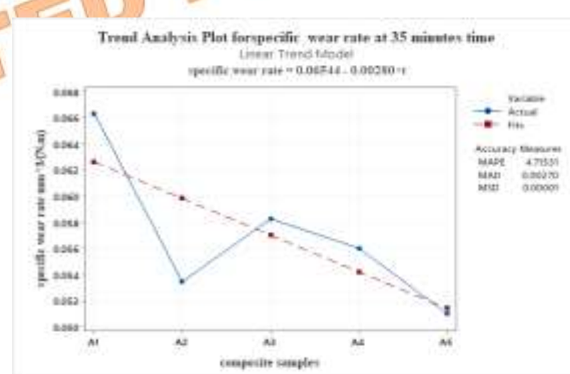

Fig. (8). The trend analysis of specific wear rate

The same results are evident in the residual plots of Fig. 9. The plot of Probability shows that the data are close to a straight line, indicating that the experimental results are normally distributed with no bias in the testing results. The residual-versus-fitted value curves show that the differences in specific wear rates are randomly distributed around the line of zero value; this means that the specific wear rate experimental data model fits the data very well, with linearity and constant-variance residuals. Since the differences are distributed randomly around the zero line without any discernible pattern, the residuals are independent and identically distributed, meeting the model assumptions from experimental testing results in the residual-versus-observation plots showing an accurate model.

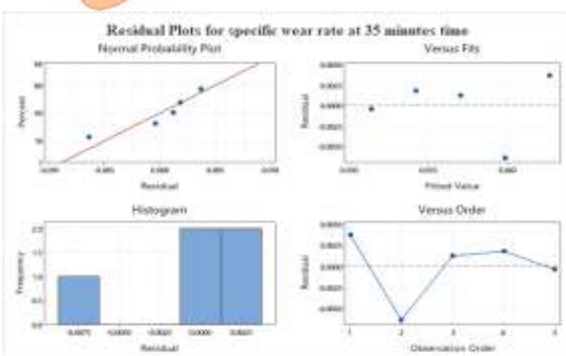

Fig. (9). The residual plots of specific wear rate

Figure 10 below shows the trends in specific wear rate over time for the three trend analysis equations.

Over time, the specific wear rate at a load of 15 N decreased very slowly from the initial 0.000655, with a decrease of 0.000019 units per unit increase in time, indicating a negative linear trend, suggesting that the addition of ZnO enhances the tribological characteristics of the composite.

At 25 N, the specific wear rate increases gradually. The initial wear rate is 0.03895 and 0.000532 units per unit increase in time, showing a positive linear trend with time. The composite material endures a higher applied load, leading to greater contact area and increased wear, while the hard particles of poorly bonded SiC play a key role in causing a micro-ploughing effect on the surface.

Increasing the applied load to 35 N resulted in a noticeable decrease in the specific wear rate over time. The initial wear rate is 0.065, and the decrease of 0.0028 units per time in the time trend equation is a much faster rate than the 25 N specific wear rate. This caused a negative linear trend. The rapid decrease in wear rate is due to the significant effect of reinforcement addition to the Aluminum metal and the surface smoothing with increased applied load, leading to increased contact areas with lower contact stresses and, as a result, a reduction in wear rate [27].

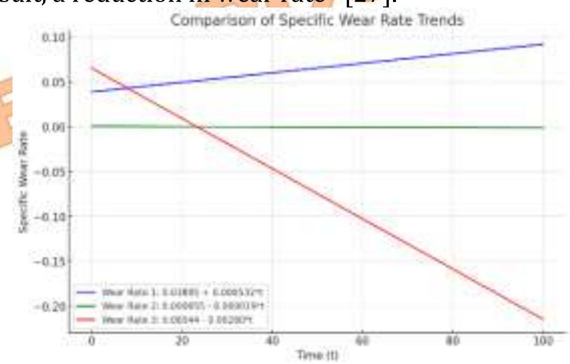

Figure (10) the specific wear rate trends with time comparison for the three trend analysis equations

Brinell hardness results are shown in Fig. 11. Al reinforced with SiC has a small indentation diameter and hardness due to the hard ceramic particles of SiC. ZnO imparts hardness to Al in smaller amounts[28]. Hybrid reinforcement of SiC and ZnO showed a noticeable decrease in hardness, which might be attributed to the poor distribution of the reinforcement particles. To clearly visualize the hybrid composite hardness, further verification through subsequent microstructural characterization is needed [29].

In the hybrid composite, the highest hardness is obtained when the maximum amounts of SiC and ZnO are combined in the A5 sample.

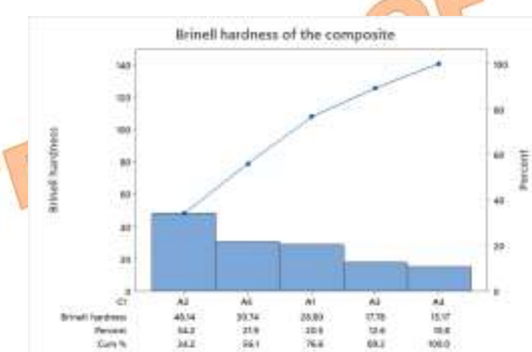

Fig. (11). Brinell hardness results of the composite materials

5. Finite Element Analysis

5.1. Static Structural Analysis

The Finite Element method is a widely used technique for simulating and analyzing the behavior of complex structures under varying applied conditions. FEM. Permits engineers to predict performance, identify failure points, and improve material performance when applied to the design and improvement of hybrid composite materials [30]. The disk brake 3D geometry model was built in SolidWorks 22. The analysis was performed in ANSYS 2022 R1 Workbench [ANSYS, Inc., Canonsburg, PA, USA] by importing an IGS file from SolidWorks. The disk brake 3D element with 10 nodes (isoperimetric) has a meshed model with 14610 nodes and 7746 elements. Ansys model mesh was selected for the principal study of structural behavior of the model and to ensure numerical stability while keeping realistic computational cost[31]. For more accurate results of stress around holes and edges, the mesh is systematically refined.
The disk brake rotational velocity was 125 rpm, and the applied load was 15- 35 N, which do not represent the maximum loads that the disk brake may experience, but rather a reliable measurement of the hybrid disk brake functional integrity and service life.

The linear velocity was around 30 km/ hr. to study low -speed braking conditions. At this velocity, the braking first cycle initial contact pressure and thermal distribution were investigated. All bolt holes were loaded as fixed support. The hybrid composite disk brake model constraints and meshed model are shown in Fig. 12.

Fig. (12). ANSYS constraints, model, and meshing of the disk brake

Table 3 shows the Geometrical specification and structural properties of the 3D model of the disk brake.

Table 3. Geometrical specification and structural properties of 3D model of disk brake

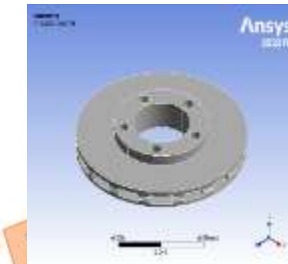

Item	values
Max. compressive strength MPa	820
Disk volume m^3	3.4558e-004
Mass kg	2.7128
Elastic modulus, GPa	145
Outer disk diameter, mm	200
Inner disk diameter, mm	70
Disk thickness, mm	30
Diameter of central 5 holes, mm	12

Using the hybrid composite materials sample A5 test results (having the best properties) as input, perform static structural analysis in ANSYS 2022 R1 Workbench to evaluate the stress, deformation, strain, and thermal behavior of the hybrid composite disk brake.

5.2. Steady-state Thermal Analysis

The hybrid disk brake's steady-state thermal behavior was studied by exposing the A5 hybrid composite disk brake to 100 °C at the disk surfaces, simulating steady-state, light braking, and non-severe operating conditions where thermal equilibrium is assumed in everyday service city driving. This assumption simulates temperatures during rotation for comparative evaluation of material thermal responses rather than precise simulation of real braking heat conditions.

The convection at the holes and the inner diameter of the disk, with tabular convection coefficients for stagnant air, are used in the horizontal cycle. The model material, geometry dimensions, and meshed model characteristics are

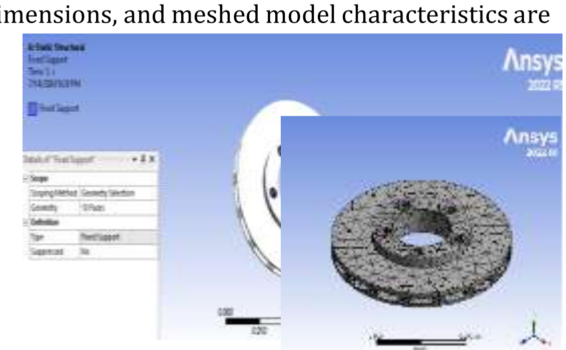

the same as in the static structural model. The applied thermal loads, temperature, and convection load are shown in Fig. 13 below. The experimental constraints were chosen to simulate moderate city decelerating environments.

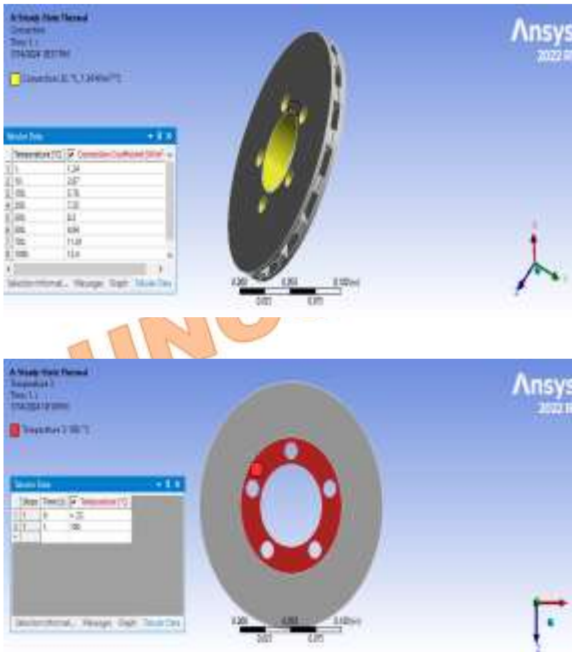

Fig. (13). Thermal loads of the hybrid composite disk brake.

6. Finite Element Results

6.1. Static Structural Results

Figure 14 shows that the highest equivalent von Mises stress of the hybrid composite is 1.29 MPa. Although this stress is low, it is considered acceptable for evaluation of disk brake stability rather than its ultimate failure. The smallest value is 2781.5 Pa at the outer surfaces and the fixed supports. The radial and tangential stresses vary with radius at the rotating disk; they are much lower than those at the inner radius surfaces.

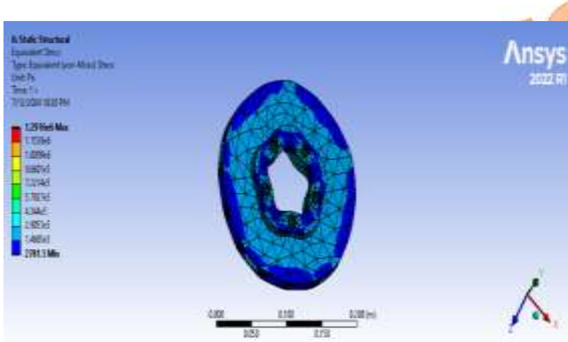

Fig. (14) Von Mises stress of the hybrid composite disk brake.

The total deformation in Fig. 15 shows that the maximum deformation occurs at the outer diameter, adjacent to the fixation points. This may be attributed to the supports, which restrict motion while the rotational velocity is applied to the disk [32].

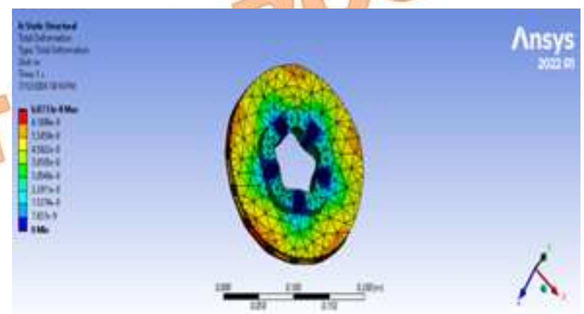

Fig. (15). Total deformation of the hybrid composite disk brake.

The smallest elastic strain energy is at the outer diameter of the disk brake, as shown in Fig. 16, because, under operational conditions, stress and deformation are distributed, as the outer diameter experiences fewer constraints and stresses.

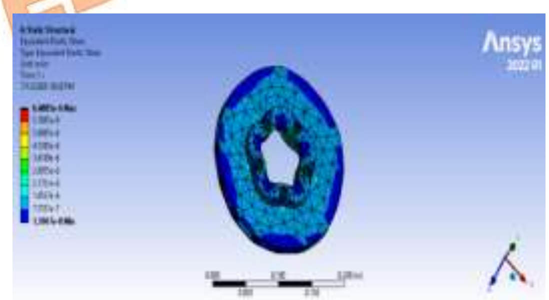

Fig. (16) Equivalent elastic strain of disk brake composite.

6.2. Finite Element Thermal Results

Figure 17 shows that the disk brake's maximum temperature at the outer surface is 100.25 °C. This surface is in direct contact with the brake pads during braking, which generates frictional heat. The inner surfaces exhibit temperature variations at different rates due to the presence of cooling channels, and structural features affect the uniform distribution of temperature [15].

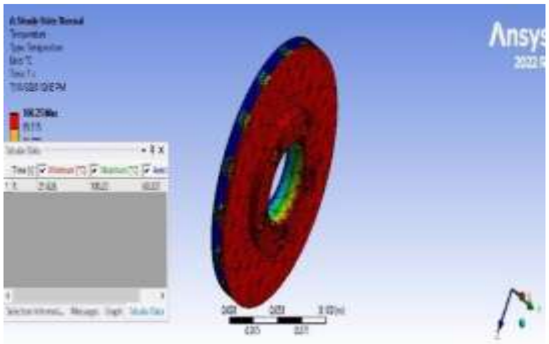

Fig. (17). Temperature distribution of the hybrid composite disk brake

The steady-state thermal total heat flux is shown in Fig. 18 below. During rotation, the outer surfaces of a larger radius of rotation experience higher linear velocity, which enhances frictional heating and increases heat flux[33].

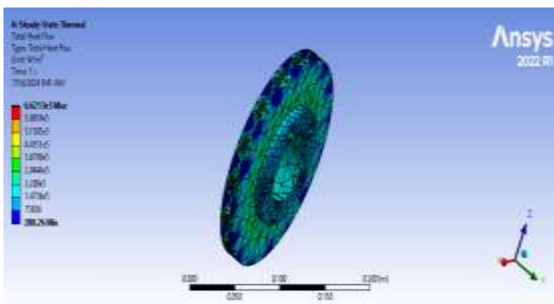

Fig. (18). Total heat flux of the hybrid composite disk brake

Figure 19 shows steady-state directional heat flux. The outer surfaces exhibit a uniform distribution of average heat flux. Directional heat flux shows a slight increase near the inner radius, the disk protrusions, and edges. The cooling channels have a heat flux distribution higher than other surfaces because of the exposure to the outer environment and air flow [34].

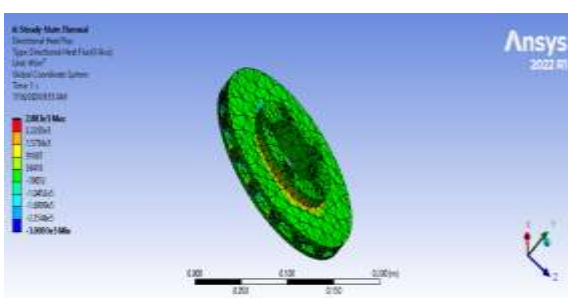

Fig. (19). Steady-state directional heat flux of the composite disk brake

7. Conclusions

The study was performed to estimate the viability of developing high-performance hybrid composites for automotive braking applications. Performing the experimental testing with statistical optimization through Minitab and advanced numerical validation using ANSYS Workbench, the research provided a wide-ranging evaluation of how hybrid reinforcements impact the mechanical properties, wear, and thermal characteristics of disk brakes.

Establishing resistance to wear as an important test in disk brake manufacturing, the hybrid composite A5 has the best resistance to wear rate, which is the strongest formulation among the tested samples.

Time trend analysis of Minitab 19 further validated these findings. This certified A5 as the optimum structural stability over time sample, and the best material for hybrid disk brake manufacturing.

The mechanical and thermal behavior of the design were explored by ANSYS static numerical investigation of stress, strain, and deformation. The numerical results provided serious understanding of which stress levels are significantly lower at the outer surfaces compared to the inner regions, signifying a necessity for localized reinforcement in the new designs. The thermal analysis showed that maximum temperatures are maximized at the disk surface, with the inner surfaces having higher heat flux concentration. The obtained results verify that the development of hybrid composites, precisely the A5 formation, provides a feasible path for improving the competence, thermal control, and active lifetime of automotive braking systems.

Considering the above conclusions and to integrate the study in this subject, different percentages of zinc oxide could be studied while keeping the silicon carbide percentage at 25 wt.%. The transient analysis would be proposed to compare the mechanical properties with those of the static analysis of the hybrid composite disk brake.

Acknowledgments

No Acknowledgments

Funding Statement

No Funding Statement

Conflicts of Interest

No Conflicts of Interest

Appendixes

No appendixes

References

[1]. Pind, R. R., & Swami, P., 2016. Analysis and Computational Investigation of Brake Disc for Composite Materials. *International Journal of Engineering Development and Research*, 4(4), pp.927-946.

[2]. Kader, E. E., Abed, A. M., Radojković, M., Savić, S., Milojević, S., & Stojanović, B. ,2025. Design of a Copolymer-Reinforced Composite Material for Leaf Springs Inside the Elastic Suspension Systems of Light-Duty Trucks. *Journal of Composites Science*, 9(5), pp. 1-21.

[3]. Sarip, S.,2013. Design Development of Lightweight Disc Brake for Regenerative Braking–Finite Element Analysis. *International Journal of Applied Physics and Mathematics*, 3(1), pp.52–58.

[4]. V, M. T., & M, S. P., 2007. Structural and Thermal Analysis of Rotor Disc of Disc Brake. *International Journal of Innovative Research in Science, Engineering and Technology*, 2(12), 7741–7749.

[5].Kuciej, M., & Grzes, P. 2011. The Comparable Analysis of Temperature Distributions Assessment in Disc Brake Obtained Using Analytical Method and F.E. Model. *Journal of KONES Powertrain and Transport*, 18(2),pp. 235–250.

[6]. Surendran, R., Kumaravel, A., & Sarathiperumal, S., 2014., Development and Investigation of Aluminium Metal Matrix Composite Reinforced with Silicon Carbide Particulate for Automobile Brake Disc Application. Journal of Research in Aeronautical and Mechanical Engineering, 2(4), pp.53-60.

[7]. Casamassa, E., Fioravanti, A., Mazzocchi, M., Carotta, M. C., & Faga, M. G. 2020. Abrasive properties of ZnO: Influence of different nanoforms. *Tribology International*, 142(2020), 105984.

[8]. Grzes, P., 2019. Maximum temperature of the disc during repeated braking applications. *Advances in Mechanical Engineering*, 11(3), 1–13.

[9]. Pohane, R. K., Kongare, S. C., & Daf, S. P., 2016. Mechanical Property Which Affect the Performance of Disk Brake Material, 4(20), pp.1-5.

[10]. Niranjan, H. B., 2012. Influence of Fiber Orientation and Thickness on Tensile Properties of Laminated Polymer Composites. *Int. J. Pure Appl. Sci. Technol,* 9(1), pp. 61-68.

[11]. Wankhade, L. N., Rathod, D., Nukulwar, M. R., Agrawal, E. S., & Chavhan, G. R. ,2021. Characterization of aluminium-silicon carbide metal matrix composites. *Materials Today: Proceedings*, 44(2), 2740–2747.

[12]. Abu Bakar, Abd. R., & Quyang, H. ,2012. Prediction of Disc Brake Contact Pressure Distributions by Finite Element Analysis. *Jurnal Teknologi*, 43(A), pp. 21–36.

[13]. Huajiang, O., & Abd Rahim, A.-B. ,2008. recent studies of car disk brake squeal. *In: New Research on Acoustics*, 372(1),pp.159-198.

[14]. Mahmood Ghauri, K., Ali, L., Ahmad, A., Ahmad, R., Meraj Din, K., Ahmad Chaudhary, I., & Abdul Karim, R., 2013. Synthesis and Characterization of Al/SiC Composite Made by Stir Casting Method. *In J. Engg. & Appl. Sci* ,12 (jan.), pp. 102- 110.

[15]. Khalanisohil et.al. ,2016. Design and thermal Analysis of Disc Brake using Ansys. *ARDIJEET*, 4(4), 1–10.

[16]. Kumar, S. M., & Gopala Krishna, S. G.,2014. Study on Effect of Thickness and Fibre Orientation on a Tensile and Flexural Properties of a Hybrid Composite. *Journal of Engineering Research and Applications*, 4(8), pp.56–66.

[17]. Kale, C., & Kesheorey, P. ,2019. DESIGN AND ANALYSIS OF DISC BRAKE. *IJRTI*, 4(5), pp.98-101.

[18]. Kader, E. E., & Abed, A. M.,2025. Optimization of ceramic composite material disk brakes design for automotive applications: A study on lightweight structure, efficiency, and mechanical durability. Proceedings of the Institution of Mechanical Engineers, *Part D: Journal of Automobile Engineering,0(0),* https://doi.org/10.1177/09544070251345118.

[19]. Nathan, C., Wadai, J., & Jones, N. D., 2021. Development of Brake Pad Using the Locally Available Materials. *International Research Journal of Engineering and Technology*, 8(7), pp. 2395-0072.

[20]. Kader, E. E., Asaad, L. M., & Abed, A. M.,2020. Structural properties of Epoxy-polysulfide copolymer reinforced with silicon carbide powder. In Journal of Mechanical Engineering Research and Developments, 44(4), pp. 289-295

[21]. Mohit Mittal. ,2015. Application of Taguchi Method for Optimization of Process Parameters in Improving the Productivity of Corrugation Operation. *International Journal of Research*, 2(10), pp. 537–545.

[22]. Kadhim, E., Edan, E., & Yousuf, L.,2020. Comparison study of damping analysis of hybrid composite friction disc clutch. *AIP Conference Proceedings*, 2213(020144),pp.1-7

[23]. Miladinović, S., Veličković, S., & Novaković, M. ,2016. Application of Taguchi Method for the Selection of Optimal Parameters of Planetary Driving Gear. *In Applied Engineering Letters* ,1(4). pp. 98-104.

[24]. Kumar, V. V., & Kumaran, S. S. ,2019. Friction material composite: Types of brake friction material formulations and effects of various ingredients on brake performance-a review. *In Materials Research Express* ,6(8), pp.1-27.

[25]. Onyenanu, I. U., & Nwigbo, S. C.,2021. Optimization of Aluminium Metal Matrix Composite (AMMC) for use in Automobile Brake Disc. *International Journal of Engineering Research & Technology,* 10(7), pp. 634 -638.

[26]. Duong, T. G.,2023. Application of the Taguchi Method to Determine Optimized Parameters for Designing Brake of Hand Winch. *EUREKA, Physics and Engineering*, 6(1), pp. 137–148.

[27]. Edan, E., & Al-Ezzi, A. S. (n.d.). Optimization and Analysis of Sic-Reinforced Copolymer Blend Composite Structural Springs*. Proceedings of the Institution of Mechanical Engineers, Part E: Journal of Process Mechanical Engineering*. 239(5), pp.2794-2804.

[28]. Kheradmand, A. B., Fattahi, M. R., Tayebi, M., & Hamawandi, B.,2022. Tribological Characterization of Reinforced Fe Matrix Composites with Hybrid Reinforcement of C, Cu, and SiC Particulates. *Crystals*, 12(5), pp.1-22.

[29]. Edan Kader, E., Adwan, R., & Yousuf Zedan, L.,2020. Fabrication of hybrid composite materials leaf spring. *Journal of Mechanical Engineering Research and Developments* ,44(2), pp. 132-140.

[30]. Loganathan, T. G., Vinoth Kumar, K., & Madhu, S.,2020. Flexural and fatigue of a composite leaf spring using finite element analysis. *Materials Today: Proceedings*, 22 (2020), pp.1014–1019.

[31]. Ivan Palinkas1, J. P. E. D. A. R. D. N.,2025. Analysis and Optimization of UAV Frame Design for Manufacturing from Thermoplastic Materials on FDM 3D Printer*. Material Plastic,* 62(3), pp. 72–83.

[32]. Ajeet Kumar Rai, R. R. P.,2015. structural Design and Analysis of Disc brake in Automobiles. *Journal of Mechanical Engineering Research and Developments* ,45(3), pp. 132-140.

[33]. Agnihotri, V., & Chopra, M. K. (n.d.). Optimized Thermo-Structural Analysis of Solid and Vented Disc Brake Using Finite Element Method (A Case Study). In IOSR Journal of Mechanical and Civil Engineering *JMCE*, 11(4), pp. 40- 49.

[34]. Bhatwadekar, S., & Kulkarni, P. G. R. ,2017. Design, ANALYSIS and Optimization of Brake Disc Made of Composite Material for A Motor Cycle. *International Journal of Research Publications in Engineering and Technology 3*(3), pp. 63- 69.